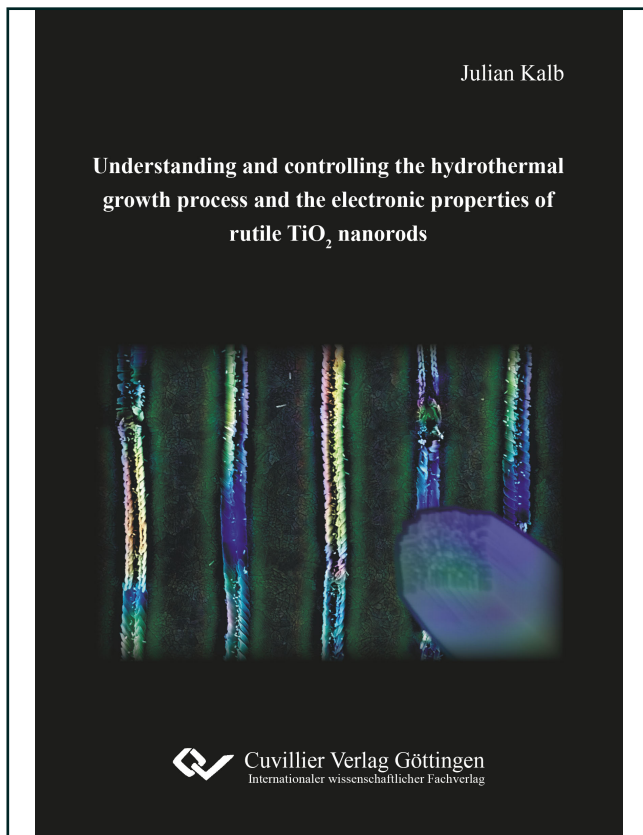




Julian Kalb (Autor)

**Understanding and controlling the hydrothermal growth process and the electronic properties of rutile TiO<sub>2</sub> nanorods**



<https://cuvillier.de/de/shop/publications/8149>

Copyright:

Cuvillier Verlag, Inhaberin Annette Jentsch-Cuvillier, Nonnenstieg 8, 37075 Göttingen, Germany

Telefon: +49 (0)551 54724-0, E-Mail: [info@cuvillier.de](mailto:info@cuvillier.de), Website: <https://cuvillier.de>



# Contents

<b>Abstract</b>	<b>1</b>
<b>1 Introduction</b>	<b>5</b>
<b>2 Basics of Titanium Dioxide</b>	<b>11</b>
2.1 Exploitation and Economic Meaning of TiO <sub>2</sub>	11
2.2 Crystal Properties of Rutile and Anatase TiO <sub>2</sub>	15
2.2.1 Morphologies and Crystal Structure	15
2.2.2 Crystal Defects	16
2.2.3 Surface Science of TiO <sub>2</sub>	17
2.2.4 Crystal Dynamics and Thermal Properties	18
2.3 Phase Transitions in TiO <sub>2</sub> /Substrate Systems	23
2.3.1 Anatase-to-Rutile Phase Transition in Bulk TiO <sub>2</sub>	23
2.3.2 Anatase-to-Rutile Phase Transition in Nanocrystalline TiO <sub>2</sub>	28
2.4 Extended Definition of Optical, Electronic, and Optoelectronic Properties of TiO <sub>2</sub> Semiconductors	37
2.4.1 Optical Properties	38
2.4.2 Electronic Properties	38
2.4.3 Optoelectronic Properties	39
2.5 Optical Properties of TiO <sub>2</sub>	40
2.5.1 Refractive Index and Dielectric Function	40
2.5.2 Light Scattering on Spherical TiO <sub>2</sub> Nanoparticles	42
2.5.3 Dielectric Light Scattering on Highly Anisotropic Nanoparticles	43
2.5.4 An Ordered Array of Nanoparticles as a Basic Module of Metamaterials	45
2.5.5 Disordered Assemblies of Nanoparticles as an Effective Medium	46
2.6 Electronic Properties of Bulk and Nanostructured TiO <sub>2</sub>	47
2.6.1 Band Structure in Bulk TiO <sub>2</sub>	47
2.6.2 Chemical Potential and Electron Density in Intrinsic Semiconductors	48
2.6.3 Chemical Potential and Electron Density in n-type TiO <sub>2</sub>	49
2.6.4 Band-Derived Effective Mass of Electrons	50
2.6.5 Conductivity and Mobility of Electrons in TiO <sub>2</sub>	50
2.6.6 Electronic States and Conductivity in Doped TiO <sub>2</sub>	60
2.6.7 Electronic States and Conductivity on Surfaces and Grain Boundaries in TiO <sub>2</sub>	68
2.6.8 Electronic States and Conductivity in TiO <sub>2</sub> Nanoparticles	71
2.7 Static Transient Current Effects in TiO <sub>2</sub>	75
2.7.1 Band Bending at the Metal-Semiconductor Interface	75
2.7.2 Electrode-Limited Conduction Mechanisms	81
2.7.3 Bulk-Limited Conduction Mechanisms	84
2.7.4 Effects of Structure Size on the Transient Current	91
2.7.5 Effects of the Fabrication Technique on the Transient Current	92
2.7.6 Effects of Post-Treatment on the Transient Current in TiO <sub>2</sub>	92



2.8	Time-Dependent Transient Current Effects in TiO <sub>2</sub> . . . . .	95
2.8.1	Capacitive Effects . . . . .	96
2.8.2	Inelastic Electron-Phonon Scattering and Joule Heating . . . . .	97
2.8.3	Trapping and Detrapping of Electrons . . . . .	98
2.8.4	Drift Velocity Effects . . . . .	101
2.8.5	Oxide Degradation . . . . .	101
2.8.6	Localized Resistive Switching Behavior . . . . .	106
2.8.7	Effect of Adsorbates . . . . .	107
2.9	Optoelectronic Properties of TiO <sub>2</sub> . . . . .	109
2.9.1	Excitation of Optical Phonons . . . . .	109
2.9.2	Excitation of Bound Charge Carriers . . . . .	109
2.9.3	Electron Injection via Adsorbates . . . . .	112
2.9.4	Light-Controlled Density of Mobile Electrons . . . . .	112
2.9.5	Excitation of Mobile Electrons . . . . .	113
2.9.6	Photoconductivity and Photocurrent . . . . .	113
2.9.7	Internal Photoemission . . . . .	113
<b>3</b>	<b>Manufacturing of TiO<sub>2</sub> Nanostructures</b> . . . . .	<b>115</b>
3.1	Thin TiO <sub>2</sub> Films . . . . .	115
3.1.1	Sputter Deposition . . . . .	115
3.1.2	Laser Ablation . . . . .	115
3.1.3	Electron-Beam Evaporation . . . . .	116
3.1.4	Spray Pyrolysis . . . . .	116
3.1.5	Sol-gel Method . . . . .	117
3.1.6	Atomic Layer Deposition . . . . .	117
3.1.7	TiCl <sub>4</sub> Treatment . . . . .	117
3.2	Hydrothermal Growth of Rutile TiO <sub>2</sub> Nanorods . . . . .	118
3.2.1	The Conversion of the Precursor into TiO <sub>2</sub> . . . . .	118
3.2.2	The Rutile TiO <sub>2</sub> Crystal Shape at Thermodynamic Equilibrium Condition . . . . .	120
3.2.3	Formation of Branches . . . . .	120
3.2.4	Substructure of Full-grown TiO <sub>2</sub> Nanorods . . . . .	121
3.2.5	Substrates for the Hydrothermal Growth of Rutile TiO <sub>2</sub> Nanorods . . . . .	123
3.2.6	Toxicity of the Investigated TiO <sub>2</sub> Nanostructures . . . . .	123
<b>4</b>	<b>Experimental Methods</b> . . . . .	<b>125</b>
4.1	Fabrication Techniques . . . . .	125
4.1.1	Substrates . . . . .	125
4.1.2	Rutile and Anatase TiO <sub>2</sub> Films/ Seed Layers . . . . .	125
4.1.3	Hydrothermal Growth of Rutile TiO <sub>2</sub> Nanorods . . . . .	129
4.1.4	Lithography . . . . .	129
4.1.5	Fabrication of Polystyrene Sphere Monolayers (PSML) . . . . .	131
4.1.6	Focused Ion Beam (FIB) Milling . . . . .	132
4.1.7	Scanning Probe Lithography . . . . .	132
4.1.8	Laser Lithography . . . . .	132
4.2	Characterization Techniques . . . . .	133
4.2.1	Standard Characterization Techniques . . . . .	133
4.2.2	Electronic Properties . . . . .	135
4.2.3	Optical Properties . . . . .	136



<b>5</b>	<b>Thin TiO<sub>2</sub> Films and Seed Layer for the Hydrothermal Method</b>	<b>139</b>
5.1	Thin Anatase TiO <sub>2</sub> Seed Layers . . . . .	140
5.1.1	Anatase Polycrystalline TiO <sub>2</sub> Films Made by Sputter Deposition . . . . .	140
5.1.2	Anatase Polycrystalline TiO <sub>2</sub> Films Made by Spray Pyrolysis . . . . .	144
5.1.3	Anatase Polycrystalline TiO <sub>2</sub> Films Made by SALD . . . . .	144
5.2	Thin Rutile TiO <sub>2</sub> Seed Layers . . . . .	145
5.2.1	Polycrystalline Rutile TiO <sub>2</sub> Films Made by Sputter Deposition . . . . .	145
5.2.2	Polycrystalline Rutile TiO <sub>2</sub> Films Made by Electron-Beam Evaporation . . . . .	146
5.2.3	Polycrystalline Rutile TiO <sub>2</sub> Films Made by a Sol-gel Method . . . . .	148
<b>6</b>	<b>Hydrothermal Growth of Rutile TiO<sub>2</sub> Nanorods on Rutile and Anatase Films</b>	<b>149</b>
6.1	Hydrothermal Growth in Solution . . . . .	150
6.2	Hydrothermal Growth on Rutile Seed Layers . . . . .	153
6.2.1	Hydrothermal Growth on Macroscopic Rutile TiO <sub>2</sub> Single Crystals . . . . .	153
6.2.2	Hydrothermal Growth on Sputtered, Sol-gel, and Evaporated Rutile TiO <sub>2</sub> Seed Layers . . . . .	157
6.2.3	Hydrothermal Growth on Rutile FTO Seed Layers . . . . .	159
6.3	Hydrothermal Growth on Anatase Seed Layers . . . . .	160
6.3.1	Hydrothermal Growth on Sputtered Fine-Grained Anatase TiO <sub>2</sub> Seed Layers . . . . .	160
6.3.2	Hydrothermal Growth on Coarse Grain Sputtered and Sprayed Anatase TiO <sub>2</sub> Seed Layers . . . . .	161
6.4	Stages of the Hydrothermal Growth Process . . . . .	164
6.4.1	Nucleation . . . . .	164
6.4.2	Period of Crystal Growth . . . . .	165
6.4.3	Ostwald Ripening . . . . .	166
6.4.4	One- and Multi-directional Growth (Branching) . . . . .	167
<b>7</b>	<b>Non-Equilibrium Growth Model for Fibrous Rutile TiO<sub>2</sub> Nanorods</b>	<b>171</b>
7.1	Model for the Origin of the Typical Fine Structure in Rutile TiO <sub>2</sub> Nanorods . . . . .	172
7.1.1	Facet-Dependent Crystallization Speeds . . . . .	172
7.1.2	Facet-Dependent Growth Speeds Corresponding to Wulff Construction . . . . .	172
7.1.3	Non-Equilibrium Growth Model Describing the Origin of the Fine Structure . . . . .	172
7.1.4	From Polycrystalline Fine Structure Towards Single Crystal . . . . .	174
7.2	Observable Consequences of the Non-Equilibrium Growth Model . . . . .	175
7.2.1	Attachment of Fingers . . . . .	175
7.2.2	Dependence of the Finger's Diameter on the Process Temperature . . . . .	177
7.2.3	Post-Growth Atomic Rearrangement in Hydrochloric Acid . . . . .	178
7.2.4	Post-Growth Annealing in Different Atmospheres . . . . .	179
<b>8</b>	<b>Expanding the Horizon of Position-Controlled Hydrothermal Growth Methods</b>	<b>183</b>
8.1	From Standard Methods to New Advanced Lithography Techniques . . . . .	184
8.2	Confined TiO <sub>2</sub> NRAs Made by Optical Contact Lithography . . . . .	184
8.2.1	Standard Structures . . . . .	184
8.2.2	Levitating TiO <sub>2</sub> NRAs . . . . .	184
8.3	Double Superlattice by Optical Lithography and PSML . . . . .	185
8.4	Confined TiO <sub>2</sub> NRAs Made by Electron-Beam Lithography . . . . .	188
8.5	Focused Ion Beam Triggered Growth of TiO <sub>2</sub> Nanorods . . . . .	189
8.5.1	Focussed Ion Beam Milling . . . . .	189
8.5.2	Confined NRAs Made by Focused Ion Beam Milling . . . . .	190



8.6	Advanced Scanning Probe Lithography Using Anatase-to-Rutile Transition of Localized Nanoparticles . . . . .	193
8.6.1	Advanced Scanning Probe Lithography . . . . .	194
8.6.2	Excluding Competing Processes Resulting in Localized Growth of Nanorods	194
8.6.3	Special Features of the Presented Advanced Scanning Probe Lithography	196
<b>9</b>	<b>LASER-Induced Position-Controlled Hydrothermal Growth</b>	<b>199</b>
9.1	Basics about Laser Lithography Techniques . . . . .	199
9.1.1	Formation of Interlayer between TiO <sub>2</sub> and Silicon Substrates . . . . .	199
9.1.2	Light In-Coupling in Anatase and Rutile TiO <sub>2</sub> Films . . . . .	201
9.1.3	Absorption of Incident Light . . . . .	208
9.1.4	Heat Dissipation in the Silicon/TiO <sub>2</sub> Interface Region . . . . .	209
9.1.5	Melting Parameters . . . . .	210
9.1.6	Recrystallization Process . . . . .	211
9.2	Results and Discussion of Laser Lithography Techniques . . . . .	213
9.2.1	Laser-Induced Oxidation Lithography . . . . .	213
9.2.2	cw Laser-Induced Melting Lithography (CiMeL) . . . . .	215
9.2.3	High Energy cw Laser-Induced Melting Lithography (HELM) . . . . .	215
9.2.4	Low Energy cw Laser-Induced Melting Lithography (LELM) . . . . .	217
9.2.5	Pulsed Laser-Induced Pattern Generation . . . . .	219
<b>10</b>	<b>Optical Properties of Rutile TiO<sub>2</sub> Nanostructures</b>	<b>237</b>
10.1	Scattering of Individual TiO <sub>2</sub> Nanorods . . . . .	240
10.1.1	Polarization-Dependent Scattering on Individual Nanorods . . . . .	241
10.1.2	Size Effects on Light Scattering . . . . .	242
10.1.3	Increasing Light Scattering with the Orientation of Nanorods . . . . .	244
10.2	Scattering Superlattices Fabricated with Optical Contact Lithography . . . . .	244
10.2.1	Scattering at Levitating NRA Membranes . . . . .	244
10.3	Scattering on Narrow Linear NRA . . . . .	247
10.3.1	Scattering at Superlattices Fabricated with Electron-Beam Lithography . . . . .	247
10.3.2	Scattering Superlattices Fabricated by Scanning Probe Lithography . . . . .	250
10.3.3	Scattering at Laser-Fabricated Superlattices . . . . .	252
<b>11</b>	<b>Time Evolution of the Transient Current in TiO<sub>2-x</sub> Nanocrystals</b>	<b>255</b>
11.1	General Model for the Electron Transport in As-Grown Rutile TiO <sub>2-x</sub> Nanorods . . . . .	257
11.1.1	Separating the Rod into an Upper and a Bottom Part . . . . .	257
11.1.2	The Effect of CVS on the Electronic Landscape . . . . .	258
11.1.3	A Simplified Model for $I - V$ Measurements . . . . .	261
11.2	General Model for the Electron Transport in Annealed Rutile TiO <sub>2-x</sub> Nanorods . . . . .	263
11.2.1	The Effect of Annealing in Vacuum on the Electronic Landscape . . . . .	263
11.2.2	The Effect of Annealing in Oxygen on the Electronic Landscape . . . . .	263
11.3	Electron Transport in Specific Structures . . . . .	265
11.3.1	Rutile TiO <sub>2-x</sub> Nanorods Grown at 150 °C (NR150) . . . . .	265
11.3.2	Rutile TiO <sub>2-x</sub> Nanorods Grown at 180 °C (NR180) . . . . .	273
11.3.3	Rutile TiO <sub>2-x</sub> Nanorods Grown at 220 °C (NR220) . . . . .	277
11.3.4	Rutile TiO <sub>2-x</sub> Nanorods Grown at 180 °C and treated with hot hydrochloric acid (HCL180) . . . . .	279
11.3.5	Rutile TiO <sub>2-x</sub> Nanotubes Grown at 180 °C and etched with hot hydrochloric acid (NT180) . . . . .	281
11.3.6	TiO <sub>2-x</sub> Films Deposited via Sputter Deposition (FI) . . . . .	284



---

11.3.7 The Effect of Adsorbed Oxygen on The Transient Current . . . . .	286
<b>12 Conclusion and Outlook</b>	<b>289</b>
<b>13 Appendix</b>	<b>297</b>
13.1 Chapter 5 . . . . .	297
13.1.1 Thin Seed Layers Made of Different Rutile Materials . . . . .	297
13.2 Chapter 6 . . . . .	299
13.2.1 Hydrothermal Growth on $\text{TiCl}_4$ Treatment Processed Seed Layers . . . . .	299
13.2.2 Hydrothermal Growth on Reduced $\text{WO}_3$ Seed Layers . . . . .	299
13.2.3 Hydrothermal Growth on ALD and SALD Seed Layers . . . . .	300
13.2.4 Probing the Rutile Phase with Hydrothermal Growth . . . . .	301
13.2.5 Crystal Structure and Hydrothermal Growth on Rutile/Anatase Sand- wiches . . . . .	301
13.3 Chapter 8 . . . . .	303
13.3.1 Double Superlattice by Optical Lithography and PSML . . . . .	303
13.3.2 Applying Scratching on Reduced $\text{WO}_3$ Films . . . . .	303
13.4 Chapter 9 . . . . .	305
13.4.1 Correlation Between Provided Beam Energy and Melting Behavior for cw Laser Melting . . . . .	305
13.4.2 Suppressing Hydrothermal Growth by Intensive Electron-Beam Exposure	305
13.5 Chapter 10 . . . . .	307
13.5.1 Scattering on Superstructures Made by PSML . . . . .	307
13.5.2 Intensity Pattern Occurring Near the Nanowalls . . . . .	307
13.6 Chapter 11 . . . . .	310
13.6.1 Experimental Characteristics . . . . .	310
13.6.2 The Influence of Further Effects on the Time-Dependent Charge Transport Behavior . . . . .	317
<b>Glossary</b>	<b>319</b>
<b>List of Symbols</b>	<b>325</b>
<b>List of Acronyms</b>	<b>327</b>
<b>List of Figures</b>	<b>329</b>
<b>List of Tables</b>	<b>333</b>
<b>References</b>	<b>335</b>
<b>Subject Index</b>	<b>411</b>
<b>List of scientific Output and Projects</b>	<b>421</b>
<b>Acknowledgment</b>	<b>427</b>